



<b>Title</b>	<b>Changes in the adsorption of bisphenol A, 17<math>\beta</math>-ethinyl estradiol, and phenanthrene on marine sediment in Hong Kong in relation to the simulated sediment organic matter decomposition</b>
<b>Author(s)</b>	<b>Fei, Y; Xing, BS; Li, XY</b>
<b>Citation</b>	<b>Environmental Pollution, 2014, v. 192, p. 339-146</b>
<b>Issued Date</b>	<b>2014</b>
<b>URL</b>	<b><a href="http://hdl.handle.net/10722/202674">http://hdl.handle.net/10722/202674</a></b>
<b>Rights</b>	<b>NOTICE: this is the author's version of a work that was accepted for publication in Environmental Pollution. Changes resulting from the publishing process, such as peer review, editing, corrections, structural formatting, and other quality control mechanisms may not be reflected in this document. Changes may have been made to this work since it was submitted for publication. A definitive version was subsequently published in Environmental Pollution, 2014, v. 192, p. 339-146. DOI: 10.1016/j.envpol.2014.04.041</b>

1 Re-submitted to: *Environmental Pollution* (ENVPOL-D-14-00152)

2 Date: April 27, 2014

3

4 **Changes in the adsorption of bisphenol A, 17  $\alpha$ -ethinyl estradiol,**  
5 **and phenanthrene on marine sediment in Hong Kong in relation**  
6 **to the simulated sediment organic matter decomposition**

7 **Ying-heng Fei<sup>1,2</sup>, Baoshan Xing<sup>3</sup>, Xiao-yan Li<sup>1\*</sup>**

8 <sup>1</sup> Department of Civil Engineering, The University of Hong Kong, Hong Kong, China

9 <sup>2</sup> Water Science Research Center, Guangzhou Institute of Advanced Technology, Chinese

10 Academy of Sciences, Guangzhou, China

11 <sup>3</sup> Department of Plant, Soil and Insect Sciences, University of Massachusetts, Amherst,

12 MA, USA

13 (\*Corresponding author: phone: 852-28592659; fax: 852-28595337; e-mail: xlia@hkucc.hku.hk)

14

15 **Abstract**

16 Marine sediment with an input of particulate organic matter was incubated to simulate the  
17 early aging process. On the sediment after various incubation periods, adsorption and  
18 desorption tests were conducted for three selected organic micropollutants: bisphenol A  
19 (BPA), 17 $\alpha$ -ethinyl estradiol (EE2), and phenanthrene (Phe). The results showed significant  
20 sediment organic matter (SOM) decomposition during the incubation, and the SOM decay  
21 and transformation had a profound impact on the adsorption of organic compounds by the  
22 sediment. An increasing-delay-increasing pattern of change was observed for the SOM

23 normalized partition coefficients of EE2 and Phe. This change was accordant to the  
24 transformation of SOM from labile organics into active biomass and its microbial products,  
25 and finally into more condensed and humic-like substances. Comparison between the 3  
26 model micropollutants indicates that the chemical adsorption behaviors were mostly affected  
27 by their hydrophobic properties.

28 **Capsule:**

29 The early aging process of sediment organic matter led to an increasing-delay- increasing  
30 pattern of change for the adsorption of hydrophobic organic pollutants by marine sediment.

31 **Key words:** adsorption; endocrine disrupting chemicals (EDCs); marine sediment; sediment  
32 organic matter (SOM); SOM decomposition

33

34 **1 Introduction**

35 Sediment adsorption plays an important role in the fate of environmental pollutants in the  
36 aquatic system. Sediment organic matter (SOM) has been shown to be the most important  
37 component in the adsorption of hydrophobic organic pollutants (Chiou et al., 1979). The  
38 adsorption of organic pollutants by SOM often has a stronger affinity compared to the  
39 adsorption by mineral fractions, especially in SOM-rich soil or sediment (Cornelissen et al.,  
40 2005; Voice and Weber, 1983; Zhao et al., 2010). A partition mechanism has been adopted  
41 for nonionic organic adsorption by SOM (Chiou et al., 1979; Wang and Keller, 2009) in  
42 which the partition coefficient,  $K_d$ , is used to quantify the adsorption capacity. The amount of  
43 SOM in sediment has been shown to greatly influence the partition coefficients of  
44 environmental contaminants on marine sediment (Gao et al., 1998; Xu et al., 2008).

45        Moreover, researchers have found that the adsorption of organic contaminants by  
46 sediment is affected not only by the SOM content, but also by the chemical property of the  
47 SOM (Cornelissen et al., 2005; Weber et al., 1999). Xing and Pignatello (1997) proposed that  
48 various types of SOM in aged sediment could be compared to rubbery or/and glassy polymers  
49 in explaining the sediment adsorption behaviors. Their dual model implying the impact of  
50 SOM quality on the adsorption behaviors of sediment was supported by later studies (e.g.  
51 Ran et al., 2007; Sun et al., 2010; Yang et al., 2010).

52        However, accounting for organic decomposition in sediment, the adsorption of pollutants  
53 onto marine sediment with a rich organic input from particulate organic matter can be more  
54 complicated. Under natural conditions, major fractions of labile SOM are biologically  
55 mineralized within a few months, while more refractory fractions can be rather stable in  
56 sediment (deBruyn and Gobas, 2004). Organic decomposition transforms SOM from less  
57 stable organics into humic substances (Farnet et al., 2009; Plaza et al, 2009), which would  
58 fundamentally affecting the adsorption behavior and capacity of the sediment (Fei et al., 2011;  
59 Fei and Li, 2013). Prior studies have predicted the enrichment of chemicals in sediment  
60 during SOM mineralization by theoretical analysis (Gobas and MacLean, 2003; Johnson et al.,  
61 2001). However, few experimental studies have been conducted to prove the influence of  
62 SOM degradation and transformation on the adsorption of environmental micropollutants by  
63 the sediment. There is also a need to investigate the dynamic process of SOM decomposition  
64 and its effect on sediment adsorption. Such an issue is of great importance for estuary or  
65 marine areas such as Hong Kong and the Pearl River Delta in South China, where the  
66 sediment receives a high SOM input, e.g. from stormwater runoff, sewage discharge and  
67 mariculture activities (Wang et al., 2010). In our previous studies (Fei et al., 2011; Fei and Li,  
68 2013), laboratory experiments were conducted to simulate the aging and decomposition of  
69 SOM in artificial sediment, with flour powder as the fresh SOM input. With the SOM decay

70 during the sediment incubation, the adsorption of chemicals, including bisphenol A (BPA),  
71 nonylphenol and tetracyclines, by the sediment was found to change significantly.

72 In the present study, the influence of SOM decomposition on the sediment adsorption  
73 behavior was further investigated with following major modifications: (1) instead of artificial  
74 sediment made of sand and clay, actual marine sediment was used for the experimental study;  
75 (2) instead of flour powder (carbohydrate), fish food was selected as a better SOM to provide  
76 a mixture of various particulate organic compounds; (3) three different chemicals were  
77 selected as model micropollutants with different chemical structures and hydrophobic  
78 properties. Based on the experimental results, sound theoretical analysis was conducted and  
79 more comprehensive understanding was obtained. In addition, a conceptual model was  
80 proposed to describe the dynamic change of chemical adsorption by the sediment in  
81 connection to the SOM decomposition and transformation.

82

## 83 **2 Materials and Methods**

### 84 ***2.1 Sediment samples and sediment incubation***

85 Natural sediment was collected from depths 0 to 20 cm below the sediment surface at a  
86 site (22°18.400/114°06.500) in Victoria Harbour, Hong Kong, and the sample was stored  
87 under 4°C before use. After removing shells and gravels, the marine sediment was air-dried,  
88 ground and homogenized, and dry sediment that passed through a 200 µm sieve was collected.  
89 The organic content in the raw sediment was around 6.4%. Fish food was added as a fresh  
90 SOM input into the sediment. Dried and ground fish food pellets (Hikari Lionhead, Japan)  
91 were thoroughly mixed into the sediment at a dry weight ratio of 10%. The fish food as the  
92 fresh SOM input was mostly insoluble, and its dry mass consisted of >61% of proteins, >8%  
93 of lipids, <7% of fibers, <14% of other carbohydrates, and <10% of ashes, according to the  
94 product information.

95 The sediment with a high SOM input was incubated in water to simulate the natural  
96 decay and aging process. The sediment was placed into 30 separate glass dishes, each dish  
97 being 6 cm in diameter and 1 cm in depth, and the sediment dishes were then placed on the  
98 bottom of a large water tank. The tank was filled with 20 L of saline water made with reef  
99 salt at a salinity of 10‰, which is close to the average salinity level in Deep Bay, Hong Kong,  
100 where a large amount of SOM is received from Pearl River (Xu et al., 2010). The water in the  
101 tank was circulated and aerated to ensure a dissolved oxygen (DO) level of 5 mg/L or higher  
102 in the water over the sediment. The saline water was replaced weekly and the water  
103 temperature varied between 22-24°C. Throughout the sediment incubation process, 4 dishes  
104 of the incubated sediment were retrieved each time after different incubation periods (0, 15,  
105 33, 54, 75, 96, and 125 d). The incubated sediment samples were then air-dried and ground  
106 gently before SOM analysis and the subsequent adsorption tests.

## 107 **2.2 Sediment characterization**

108 The SOM content in a sediment sample was measured by means of LOI-550 (loss on  
109 ignition at 550°C) (Beaudoin, 2003). As a simple and reliable measurement, the LOI results  
110 have been to be consistent with the element-based organic carbon analysis (Fei et al., 2011).  
111 In brief, the sediment sample was first dried in an oven at 105°C for 1 h. After cooling and  
112 weighing, the dry solids was placed in a muffle oven and heated to 550°C for 15 min,  
113 followed by cooling and weight measurement. The loss of weight after ignition was  
114 determined as the amount of SOM in the sediment. The fraction of organic matter,  $f_{OM}$ , in the  
115 raw or incubated sediment was calculated accordingly.

116 Humic substances were extracted from the sediment samples following the method  
117 previously employed by Droussi et al. (2009). Briefly, humic matter was extracted by 0.1M  
118 KOH for 7 times, the combined extract solution was precipitated by 6M H<sub>2</sub>SO<sub>4</sub>, and the  
119 precipitate was then dissolved in 0.05M NaHCO<sub>3</sub> (pH=8.0) for analysis. Fluorescence

120 excitation and emission matrix (FEEM) was obtained by a fluorescence spectrophotometer  
121 (F-7000, Hitachi, Japan) for the emission wavelength ranging 300-600 nm with the excitation  
122 wavelength ranging 250-500 nm (Plaza et al., 2009). The absorbance at 465 nm ( $E_4$ ) and 665  
123 nm ( $E_6$ ) of the humic solution was determined by a UV-VIS spectrophotometer (Lambda 12,  
124 Perkin Elmer, USA), and the  $E_4/E_6$  ratio was then calculated accordingly.

### 125 **2.3 Model micropollutants**

126 Endocrine disrupting chemicals (EDCs) have attracted public attention in recent years  
127 due to the chronic harm they cause to the reproduction of organisms in the ecosystem (e.g.  
128 Colborn et al., 1993; Collins, 2008). Two typical EDCs, BPA and 17  $\alpha$ -ethinyl estradiol (EE2)  
129 were selected as the model chemicals for the sediment adsorption study. Another typical  
130 non-polar organic contaminant, phenanthrene (Phe), which also has been indicated with  
131 potential estrogenic activities in human colons (Van de Wiele et al., 2005), was selected as  
132 well. Table 1 summarizes the chemical properties of the model compounds, including their  
133 water solubility  $S_w$  and octanol-water partition coefficient  $K_{ow}$  values.

134 The chemicals were of analytical purity, with BPA (> 99%) purchased from Aldrich  
135 (USA), EE2 (> 98%) from Sigma (USA), and Phe (> 98%) from Aldrich (USA). All of the  
136 other chemicals and solvents used in the study were of analytical grade or better and were  
137 obtained from Sigma-Aldrich (USA). BPA, EE2, and Phe were prepared in a background  
138 solution consisting of 0.01 M  $\text{CaCl}_2$  for a basic ionic strength and 200 mg/L of  $\text{NaN}_3$  for the  
139 inhibition of microbial activities during the adsorption tests (Xing and Pan, 2010). The  
140 chemical solutions were prepared just before the adsorption experiment, and the solution pH  
141 was 7.5.

#### 142 **2.4 Adsorption experiments**

143 Adsorption tests were conducted to determine the isotherms of adsorption of the model  
144 compounds on the sediment, using 11-mL or 40-mL screw-cap vials with Teflon-lined septa  
145 (Xing and Pan, 2010; Xing and Pignatello, 1997). Briefly, a pre-determined amount of  
146 sediment was placed in a series of vials, into which a model micropollutant solution of  
147 different concentrations was subsequently added. The initial concentrations of BPA, EE2 and  
148 Phe were in the ranges of 10-50 mg/L, 0.5-5 mg/L, and 0.1-0.5 mg/L, respectively. The vials,  
149 which had nearly no headspace, were placed in a temperature-controlled shaking incubator  
150 (Polyscience, USA) at 25°C and were rotated at the rate of 130 rpm. Upon completion of the  
151 adsorption test, the sediment mixture from each vial was centrifuged at 4000 rpm for 5 min to  
152 separate the liquid from the sediment, and the pollutant concentration in the aqueous phase  
153 was measured using a high-performance liquid chromatography (HPLC).

154 The dry sediment/aqueous ratios were 0.7 g/10 mL, 0.3 g/10 mL, and 5 mg/40 mL for the  
155 BPA, EE2, and Phe, respectively. The pH level of the solutions during the adsorption tests  
156 was around 7.5. Our preliminary tests showed that the adsorption equilibrium could be  
157 achieved in 24 hr for BPA or EE2 and in 72 hr for Phe. Losses of chemicals attributable to  
158 glass wall adsorption or other causes were found to be less than 3%. Thus, the amount of the  
159 chemical adsorbed by the sediment in each test vial could be determined by the difference  
160 between the initial and final concentrations in the liquid phase.

161 After the adsorption experiment being completed, a desorption test was conducted on the  
162 same sediment. For the desorption of BPA, the aqueous solution was replaced by 10 mL of  
163 the clean background solution, and the sample vials were placed in the shaking incubator  
164 (Polyscience, USA) at 25°C. After 48 hr, the sediment and solution were separated as  
165 previously described, and the BPA concentration in the liquid phase was measured by the  
166 HPLC. For EE2 desorption, due to the HPLC detection limit, only half (5 mL) of the liquid



167 was replaced with the clean solution, with the other half (5 mL) remaining in the vial. The  
168 great hydrophobicity of Phe made its desorption into water extremely difficult. Sodium  
169 dodecyl benzene sulfonate (SDBS), a surfactant often used in soil extraction (Zhao et al.,  
170 2010), was therefore dosed (5 mL) into the sediment mixture at 10,000 mg/L for Phe  
171 desorption.

## 172 **2.5 Chemical analysis**

173 The BPA, EE2, and Phe concentrations in water were measured by an HPLC (Waters  
174 2695) with a C18 column (5  $\mu$ m, 2.1 $\times$ 150 mm) for separation and a photodiode array detector  
175 (Waters 2996) for quantification. For BPA and EE2, the mobile phase was a mixture of  
176 Milli-Q water and acetonitrile (50:50, v/v). The flow rate was set at 0.5 mL/min, and the  
177 sample injection volumes were 10  $\mu$ L for BPA and 50  $\mu$ L for EE2. Under this  
178 chromatographic condition, the BPA peak appeared at around 6 min and the EE2 peak at  
179 around 8 min. The area of the peak detected at a wavelength of 225 nm was used to quantify  
180 the amount of the chemical detected (Mnif et al., 2012). The limits of detection and  
181 quantification (LOD and LOQ) were 0.03 and 0.1 mg/L for BPA and 0.1 and 0.3 mg/L for  
182 EE2. For Phe, the HPLC program was optimized by using acetonitrile as the mobile phase at  
183 a flow rate of 0.5 mL/min. The Phe peak was obtained at around 7 min by detection at 250  
184 nm (Zhao et al., 2010). Setting the injection volume at 10  $\mu$ L, the LOD and LOQ were 0.05  
185 and 0.15 mg/L, respectively. The HPLC chromatographs for the chemical detections are  
186 shown in the Supplementary Material (SI).

## 187 **2.6 Data analysis**

188 The results obtained in the sediment adsorption and desorption tests were used to  
189 determine the adsorption and desorption isotherms. The isotherm data were arranged to fit the

190 following linear partition model (Eq. 1) and the Freundlich model (Eq. 2) (Voice and Weber,  
191 1983):

$$192 \quad q_e = K_d C_e \quad (1)$$

$$193 \quad q_e = K_F C_e^{1/n} \quad (2)$$

194 where  $C_e$  and  $q_e$  are the equilibrium concentrations of the chemical in the aqueous phase and  
195 sediment, respectively;  $K_d$  is the partition coefficient in the linear model;  $K_F$  and  $1/n$  are the  
196 affinity coefficient and curvature index, respectively, in the Freundlich equation. Microsoft  
197 Excel 2010 was used for data analysis and curve fitting. Furthermore,  $K_d$  for partition is  
198 normalized by the SOM content ( $f_{OM}$ ) to obtain the organic matter normalized partition  
199 coefficient  $K_{OM}$  (Eq. 3), i.e.

$$200 \quad K_{OM} = \frac{K_d}{f_{OM}} \quad (3)$$

201 Based on the comparison between the adsorption and desorption tests for a chemical by  
202 the sediment, an hysteresis index ( $HI$ ) can be calculated as follows (Wu and Sun, 2010),

$$203 \quad HI = \frac{K_{d(D)} - K_{d(A)}}{K_{d(A)}} \quad (4)$$

204 where  $K_{d(D)}$  and  $K_{d(A)}$  stand for the chemical partition coefficients obtained from the  
205 desorption and adsorption tests, respectively. The  $HI$  value signifies the irreversibility of an  
206 adsorption process, with  $HI = 0$  representing completely reversible adsorption and a higher  
207  $HI$  value indicating more irreversible adsorption.

208

## 209 **3 Results and Discussion**

### 210 **3.1 SOM degradation and transformation**

211 The loaded SOM, fish food pallets, degradation was well observed during the sediment  
212 incubation. The organic content in the sediment fell by 47% over 4 months (Fig. 1). The  
213 SOM decomposition could be well fitted by multi-fractional first-order kinetic equations  
214 (please refer to SI). SOM decay occurred more rapidly in the first month with a reduction of  
215 around 40% of the initial  $f_{OM}$ . SOM reduction became much slower in the following 3 months.  
216 Along with the SOM degradation, fresh SOM would be rapidly transformed into biomasses  
217 and their metabolic products (Fei et al., 2011). Subsequent to SOM biodegradation, biomass  
218 and microbial intermediate products would undergo further decay to form more condensed  
219 geo-polymers such as fulvic acid, humic acid, and humin (Farnet et al., 2009; Plaza et al.,  
220 2009).

221 Analysis on humic substances confirmed the humification-like process within the  
222 sediment aging process. As shown in Fig 2., the FEEM features a primary peak at the  
223 excitation/emission wavelength pair of 370/470 nm, and a secondary peak at around 450/540  
224 nm. The  $E_4/E_6$  ratio decreased significantly, as shown in Fig 3, indicating the accumulation of  
225 aromatic contents and the condensation of the acidic humic substances in the sediment  
226 samples (Droussi et al., 2009). Based on previous studies on organic incubation or  
227 composting (e.g. Droussi et al., 2009; Guo et al., 2013), the elemental ratios of N/C, H/C, and  
228 O/C would be increased during the organic matter decomposition process. The condensation  
229 and humification process in sediment would change SOM into more humic-like matter  
230 eventually with more carboxyl groups, alkyl carbon, and non-lignin aromatic structures  
231 (Farnet et al., 2009).

### 232 3.2 Adsorption and desorption of BPA

233 Batch adsorption tests were conducted with the model chemical compounds to  
234 characterize the change in the adsorption properties of the sediment after various periods of  
235 incubation. The isotherms of BPA adsorption by the sediment fit well with either the linear  
236 partition model or the Freundlich model ( $R^2 \geq 0.98$ ) (Table 2 and Fig. 4). Chiou et al. (1979)  
237 suggested that the adsorption of hydrophobic organic contaminants on soil or sediment could  
238 be accurately described by the linear model with a partition coefficient indicating adsorption  
239 capacity. Mathematically, the linear model can be considered a special case of the Freundlich  
240 isotherm model when the curvature index  $1/n$  in the Freundlich equation is close to 1 (Voice  
241 and Weber, 1983). To allow simple and direct comparisons, the linear isotherm model and  
242 related partition coefficients were used in most of the following analysis and discussion to  
243 mathematically compare adsorption capacity between sediment samples after different  
244 incubation periods.

245 For BPA, the partition coefficient  $K_d$  of the sediment cooperated with fish food pellets  
246 increased by 8 times than the raw sediment (Table 2). The affinity coefficient in the  
247 Freundlich model,  $K_F$ , showed more than 3 times of increase. It has been widely  
248 demonstrated that a higher SOM content would lead to a higher adsorption affinity (e.g. Fei  
249 et al., 2013; Sun et al., 2010; and Xu et al., 2008). Besides, the curvature index,  $1/n$ , also  
250 increased from 0.71 to more than 0.97. For the raw sediment, the curved adsorption isotherm  
251 has been commonly reported by others (e.g. Cornelissen et al., 2005; Gao et al., 1998; Voice  
252 and Weber, 1983; etc.), and the linearity of the sorption isotherm is usually negatively related  
253 with the SOM maturity (Cornelissen and Gustafsson, 2004).

254 For the SOM loaded and incubated sediment,  $K_d$  decreased by 69% from 35 to about 11  
255 L/kg after 4 months of incubation. Most of the  $K_d$  decrease occurred in the first month,  
256 accounting for a 54% decrease from the initial value.  $K_d$  fell by another 15% in the following

257 3 months. It is apparent that the loaded SOM influenced the adsorption capacity, and the  
258 degradation of fresh SOM was the main cause of  $K_d$  reduction, as the  $K_d$  decreases observed  
259 correlated well with  $f_{OM}$  reduction during the sediment incubation process. This is accordant  
260 to our previous findings (Fei et al., 2011; Fei and Li, 2013). However, at the end of the  
261 incubation, when the  $f_{OM}$  of the humified sediment was only 20% more than that of the raw  
262 sediment without the SOM input, the  $K_d$  was still more than doubled. The change of  
263 adsorption was not only influenced by the quantity, but also by the property. The curvature  
264 index  $1/n$  in the Freundlich model for BPA adsorption also decreased from 0.97 to 0.89,  
265 showing a more curved adsorption isotherm after SOM decay. This change is consistent with  
266 previous findings showing that the pattern of chemical adsorption by organic materials  
267 becomes more curved after organic decomposition (Hur et al., 2011; Plaza et al., 2009).

268 The desorption experiment showed that the desorption-based partition coefficient for  
269 BPA also decreased by 56% for the incubated sediment, which was still higher than the raw  
270 sediment (Table 2). Moreover, desorption hysteresis was found for BPA desorption from the  
271 sediment. Hysteresis is a result of partially irreversible adsorption, and the  $HI$  value has been  
272 used to quantify the irreversibility of chemical adsorption (Wu and Sun, 2010). The BPA  
273 desorption results indicated that  $HI$  increased continuously and significantly for the incubated  
274 sediment. The  $HI$  change also correlated well with the transformation of SOM during  
275 incubation, as chemical adsorption by condensed SOM is theoretically stronger, and chemical  
276 desorption by more condensed SOM is harder than that by less condensed SOM (Gunasekara  
277 and Xing, 2003).

### 278 **3.3 Adsorption and desorption of EE2**

279 Similar to BPA, the isotherm of EE2 adsorption by the incubated sediment also fits well  
280 with the linear partition model ( $R^2 \geq 0.95$ ) for the sediment samples after various incubation  
281 periods (Fig. 4), whilst the curvature index  $1/n$  in the Freundlich model is close to 1 (Table 2).

282 The fresh SOM into the sediment increased the adsorption affinity as well as the isotherm  
283 linearity (Table 2, raw sediment and 0 day sediment). The fish food pellets with rich contents  
284 of proteins and lipids apparently enhanced the adsorption capacity of the sediment and  
285 changed the shape of its adsorption isotherm.

286 For the change of adsorption along with the incubation time,  $K_d$  initially decreased, but  
287 recovered in the later phase. Within the first 2 months of sediment incubation, the  $K_d$  value  
288 decreased by 43%, which correlated well with the rapid  $f_{OM}$  reduction in the sediment.  $K_d$   
289 then began to increase after about 2 months of sediment incubation and eventually reached 73%  
290 of its initial value. In the later phase of sediment incubation, a large portion of the SOM  
291 would have been transformed from simple hydrocarbons and fresh biomass to more  
292 humic-like substances with more carboxylic and aromatic groups (Farnet et al., 2009). Such  
293 SOM transformation is more favorable to the adsorption of EE2 molecules by the incubated  
294 sediment, probably through  $\pi$ - $\pi$  bonds and hydrogen bonds (Yamamoto et al., 2003).

295 As the desorption  $K_d$  values obtained were lower than the corresponding adsorption  $K_d$   
296 values, the desorption HI could not be derived for EE2. Consistent with the change in the  
297 adsorption isotherm, the  $K_d$  value determined for the desorption of EE2 also decreased  
298 initially before reversing direction and increasing (Table 2). The  $K_d$  decrease was most  
299 significant in the first month, which correlated well with the rapid  $f_{OM}$  reduction observed.

### 300 ***3.4 Adsorption of Phe***

301 A much greater amount of adsorption by the sediment was observed for Phe (Table 2).  
302 Comparison between the raw sediment with SOM added sediment demonstrated that the  
303 SOM addition greatly enhanced the sorption capacity to the sediment, as the  $K_d$  value  
304 increased from 132.5 to 4430 kg/L. The  $I/n$  values for Phe were higher than 1 for some of the  
305 aged sediment. This might be contributed to multilayer adsorption, as the sediment surface  
306 would be modified by the Phe adsorption, leading to more and stronger adsorption. In

307 comparison to BPA and EE2, the partition coefficient of Phe showed a lower degree of  
308 change during the sediment incubation. Its  $K_d$  value initially increased by 11% before  
309 decreasing from 5612 on 15 day to 4686 L/Kg on 54 day (Table 2). The adsorption then  
310 began to recover, eventually reaching to a level of around 5000 L/kg. It has been reported that  
311 the sorption of Phe on SOM is mainly driven by hydrophobic effects (Wang et al., 2011). The  
312 hydrophobic carbon content (the sum of alkyl and aromatic carbon content) was expected to  
313 increase in the later phase of SOM decay in the incubated sediment (Hur et al., 2011), which  
314 would lead to more and stronger nonspecific Phe bindings by the sediment for adsorption.

315 The strong degree of Phe adsorption by the sediment meant the surfactant SDBS had to  
316 be used for the desorption tests. As a result, the partition coefficients of the desorption  
317 isotherms were much lower than those of the adsorption isotherms and hence could not be  
318 compared with the latter. Nonetheless, an increasing trend in desorption  $K_d$  became apparent  
319 as the sediment incubation progressed, which also indicated stronger Phe adsorption by the  
320 incubated sediment.

321 Data fitting with the Frunelich model showed the isotherm of Phe adsorption by the  
322 incubated sediment became more non-linear in the later phase of sediment incubation (Table  
323 2). The curvature index  $1/n$  increased from 1.02 at the beginning of the incubation period to  
324 more than 1.50 by the end. A value of  $1/n > 1$  often indicates easier and stronger partitioning  
325 at higher concentrations (Voice and Weber, 1983). It is apparent that the SOM was converted  
326 to more condensed and humic-like materials with a strong binding affinity to Phe (Grathwol,  
327 1990; Plaza et al., 2009).

### 328 **3.5 $K_{OM}$ for BPA, EE2, and Phe**

329 SOM in sediment is believed to be the main adsorbent for chemical adsorption (e.g. Sun  
330 et al., 2010; Wu and Sun, 2010; Xu et al., 2008). SOM normalized  $K_d$  was determined for the  
331 model compounds (Fig. 5) using the  $K_d$  values and  $f_{OM}$ . The average  $\text{Log}K_{OM}$  values were 2.2,

332 2.9, and 4.7 for BPA, EE2, and Phe, respectively. In other words, among the selected  
333 contaminants, BPA was in all instances adsorbed the least and Phe was adsorbed the most by  
334 the SOM after various periods of incubation. This is consistent with the common  
335 understanding that the adsorption or partition of hydrophobic contaminants correlates  
336 strongly with the hydrophobicity of the chemical molecules (Chiou et al., 1979; Voice and  
337 Weber, 1983). In comparison to EE2 and Phe, BPA has a much lower  $K_{ow}$  and a much higher  
338  $S_w$  value (Table 1), which probably gives rise to its weak affinity with sediment organics and  
339 hence its lowest level of adsorption by the sediment. Karickhoff et al. (1979) developed the  
340 following relationship between the adsorption coefficient and the adsorbate hydrophobicity,

$$341 \quad \text{Log } K_{oc} = \text{Log } K_{ow} - 0.21. \quad (5)$$

342 Based on this correlation, the  $\text{Log}K_{oc}$  values of the studied chemicals could be calculated as  
343 2.0, 3.9, and 4.4 for BPA, EE2, and Phe, respectively. Comparison between the experimental  
344  $K_{OM}$  and the predicted values, a disagreement for EE2 can be found, as the  $K_{OM}$  determined  
345 for EE2 was lower than expected. This result might have been affected by other factors,  
346 besides the hydrophobic properties, such as the molecular size and structure of the chemicals  
347 (Sun et al., 2010). For instance, the molecular size of EE2 is larger than that of BPA, which  
348 would be an impediment for EE2 molecules accessing some adsorption sites. This could be  
349 one of the more likely reasons for the difference in  $K_{OM}$  between EE2 and Phe being greater  
350 than that predicted from the  $K_{ow}$  values alone.

351 The  $K_{OM}$  values were found to undergo various changes rather than staying constant  
352 during the sediment incubation period. A general trend of increasing-delay-increasing could  
353 be used to characterize the  $K_{OM}$  values for EE2 and Phe. Despite the great difference in values,  
354 the  $K_{OM}$  for BPA, EE2, and Phe increased sharply within the first 15 days of incubation (Fig.  
355 5). This correlates well with the period when the microbial activity increased greatly in the



356 sediment, as indicated by the rapid SOM degradation (Fig. 1) in the present work and  
357 observed in our previous studies (Fei et al., 2011).

358 Afterwards, there was a slight decrease in  $K_{OM}$  for BPA and EE2, followed by a rather  
359 stable pattern of values over a long period (d 33-75). During this period, SOM decomposition  
360 became slower (Fig. 1), with biomass decay in the sediment (Fei et al., 2011). According to  
361 the analysis of humic substances (Fig. 2), the humification process was in progress, though  
362 not dramatically yet. The decrease of active biomass possibly caused the decrease of  $K_{OM}$  for  
363 BPA and EE2. However, the inconspicuous transformation of SOM fractions might offset  
364 this loss and keep the  $K_{OM}$  stable for a period.

365 Subsequently, biodegradable SOM was exhausted and biomass decay became more  
366 important, when humic-like substances accumulated remarkably in the sediment (Fig. 2)..  
367 The SOM was further converted into more condensed humic-like substances with more  
368 aromatic, phenolic, carboxyl and other functional groups (Farnet et al., 2009) with higher  
369 chemical adsorption capacities to hydrophobic chemicals (Gunasekara and Xing, 2003; Hur  
370 et al., 2011). Owing to the SOM degradation and humification,  $K_{OM}$  increased by 111% and  
371 38% for Phe and EE2, respectively (Fig. 5). Thus, SOM input and decomposition in the  
372 sediment had a profound impact on its adsorption behavior and capacity.

373 Noticeably,  $K_{OM}$  of BPA did not increase at the end, but decreased by 42% (Fig. 5). The  
374 different 'increasing' levels were found to be well consistent with the chemical  
375 hydrophobicity, following the sequence of BPA<EE2<Phe. This result was similar to that  
376 obtained by Sun et al. (2012), which reported that the adsorption of BPA, EE2, and Phe  
377 decreased, insignificant changed, and increased, respectively. For the reason that Phe might  
378 be much more dependent on the hydrophobic interactions than BPA (Sun et al., 2012), the  
379 changes in the polarity and accumulation of aromatic structures of SOM would bring much  
380 more significant effect on the increased hydrophobic adsorption to Phe. For relatively

381 hydrophilic molecules like BPA, however, the shifted SOM structure might not be able to  
382 make positive impact. As for the differences among chemicals with varied chemical  
383 properties, a conceptual model is presented in SI, which would help explain the possible  
384 changing process of sediment adsorption in relation to SOM decomposition.

## 385 **4 Conclusions**

- 386 • Fresh SOM (fish food pellets) in marine sediment was decomposed during a 4-month  
387 incubation. Extraction and analysis of humic-like substances suggest a humification-like  
388 process during the sediment and SOM incubation.
- 389 • The adsorption behaviors of the 3 model micropollutants (BPA, EE2 and Phe) was  
390 significantly influenced by the SOM decomposition. The  $K_d$  for BPA and EE2 decreased  
391 by 70% and 28%, respectively, while for Phe increased by 11%.
- 392 • Generally, a 3-stage change for  $K_{OM}$  could be summarized.  $K_{OM}$  of the model chemicals  
393 all increased at the beginning. After a period of delaying, it continued to increase for EE2  
394 and Phe. For BPA, which was less hydrophobic, the  $K_{OM}$  decreased eventually.

## 395 **Acknowledgments**

396 This study was supported by grants AoE/P-04/2004 from the University Grants Council  
397 (UGC) and ECF09/2011 from the Environment and Conservation Fund (ECF) of the Hong  
398 Kong SAR Government. The technical assistances provided by Mr. Keith C.H. Wong and Mr.  
399 Hamid Mashayekhi are highly appreciated.

400

## 401 **References**

402 Beaudoin, A., 2003. A comparison of two methods for estimating the organic content of  
403 sediments. *J. Paleolimnol.* 29, 387-390.

404 Chiou, C.T., Peters, L.J. and Freed, V.H., 1979. Physical concept of soil-water equilibria for  
405 non-ionic organic-compounds. *Science* 206, 831-832.

406 Colborn, T., Saal, F.S.V. and Soto, A.M., 1993. Development effects of endocrine-disrupting  
407 chemicals in wildlife and humans. *Environ. Health Persp.* 101, 378-384.

408 Collins, T.J., 2008. Persuasive communication about matters of great urgency: Endocrine  
409 disruption. *Environ. Sci. Technol.* 42, 7555-7558.

410 Cornelissen, G. and Gustafsson, O., 2004. Sorption of phenanthrene to environmental black  
411 carbon in sediment with and without organic matter and native sorbates. *Environ. Sci.*  
412 *Technol.* 38, 148-155.

413 Cornelissen, G., Gustafsson, O., Bucheli, T.D., Jonker, M.T.O., Koelmans, A.A. and Van  
414 Noort, P.C.M., 2005. Extensive sorption of organic compounds to black carbon, coal, and  
415 kerogen in sediments and soils: Mechanisms and consequences for distribution,  
416 bioaccumulation, and biodegradation. *Environ. Sci. Technol.* 39, 6881-6895.

417 deBruyn, A.M.H. and Gobas, F.A.P.C., 2004. Modelling the diagenetic fate of persistent  
418 organic pollutants in organically enriched sediments. *Ecol. Model.* 179, 405-416.

419 Droussi, Z., D'Orazio, V., Hafidi, M. and Ouattmane, A., 2009. Elemental and spectroscopic  
420 characterization of humic-acid-like compounds during composting of olive mill  
421 by-products. *J. Hazard. Mater.* 163, 1289-1297.

422 Farnet, A.M., Prudent, P., Ziarelli, F., Domeizel, M. and Gros, R., 2009. Solid-state (13)C  
423 NMR to assess organic matter transformation in a subsurface wetland under cheese-dairy  
424 farm effluents. *Biores. Technol.* 100, 4899-4902.

425 Fei, Y.H., Li, X.D. and Li, X.Y., 2011. Organic diagenesis in sediment and its impact on the  
426 adsorption of bisphenol A and nonylphenol onto marine sediment. *Mar. Pollut. Bull.* 63,  
427 578-582.

428 Fei, Y.H. and Li, X.Y., 2013. Adsorption of tetracyclines on marine sediment during organic  
429 matter diagenesis. *Water Sci. Technol.* 67, 2616-2621.

430 Gao, J.P., Maguhn, J., Spitzauer, P. and Kettrup, A., 1998. Sorption of pesticides in the  
431 sediment of the Teufelsweiher pond (Southern Germany)–I: Equilibrium assessments,  
432 effect of organic carbon content and pH. *Water Res.* 32, 1662-1672.

433 Gobas, F.A.P.C. and MacLean, L.G., 2003. Sediment-water distribution of organic  
434 contaminants in aquatic ecosystems: The role of organic carbon mineralization. *Environ.*  
435 *Sci. Technol.* 37, 735-741.

436 Gong, J., Ran, Y., Chen, D.Y. and Yang, Y., 2011. Occurrence of endocrine-disrupting  
437 chemicals in riverine sediments from the Pearl River Delta, China. *Mar. Pollut. Bull.* 63,  
438 556-563.

439 Guo, X.Y., Wang, X.L., Zhou, X.Z., Ding, X., Fu, B., Tao, S. and Xing, B.S., 2013. Impact  
440 of the simulated diagenesis on sorption of naphthalene and 1-naphthol by soil organic  
441 matter and its precursors. *Environ. Sci. Technol.* 47, 12148-12155.

442 Gunasekara, A.S. and Xing, B.S., 2003. Sorption and desorption of naphthalene by soil  
443 organic matter: Importance of aromatic and aliphatic components. *J. Environ. Qual.* 32,  
444 240-246.

445 Hur, J., Lee, B.M. and Shin, H.S., 2011. Microbial degradation of dissolved organic matter  
446 (DOM) and its influence on phenanthrene-DOM interactions. *Chemosphere* 85,  
447 1360-1367.

448 Johnson, M.D., Huang, W. and Weber, W.J., 2001. A distributed reactivity model for  
449 sorption by soils and sediments. 13. Simulated diagenesis of natural sediment organic  
450 matter and its impact on sorption/desorption equilibria. *Environ. Sci. Technol.* 35,  
451 1680-1687.

452 Karickhoff, S.W., Brown, D.S and Scott, T.A., 1979. Sorption of hydrophobic pollutants on  
453 natural sediments. *Water Res.* 13, 241-248.

454 Mnif, W., Zidi, I., Hassine, A.I.H., Gomez, E., Bartegi, A., Roig, B. and Balaguer, P., 2012.  
455 Monitoring endocrine disrupter compounds in the Tunisian hamdoun river using in vitro  
456 bioassays. *Soil Sediment Contam.* 21, 815-830.

457 Plaza, C., Xing, B., Fernandez, J.M., Senesi, N. and Polo, A., 2009. Binding of polycyclic  
458 aromatic hydrocarbons by humic acids formed during composting. *Environ. Pollut.* 157,  
459 257-263.

460 Ran, Y., Sun, K., Ma, X.X., Wang, G.H., Grathwohl, P. and Zeng E.Y., 2007. Effect of  
461 condensed organic matter on solvent extraction and aqueous leaching of polycyclic  
462 aromatic hydrocarbons in soils and sediments. *Environ. Pollut.* 148, 529-538.

463 Sun, K., Gao, B., Zhang, Z.Y., Zhang, G.X., Liu, X.T., Zhao, Y. and Xing, B.S., 2010.  
464 Sorption of endocrine disrupting chemicals by condensed organic matter in soils and  
465 sediments. *Chemosphere* 80, 709-715.

466 Sun, K., Jin, J., Gao, B., Zhang, Z.Y., Wang, Z.Y., Pan, Z.Z., Xu, D.Y. and Zhao, Y., 2012.  
467 Sorption of 17 $\alpha$ -ethinyl estradiol, bisphenol A and phenanthrene to different size fractions  
468 of soil and sediment. *Chemosphere* 88, 577-583.

469 Van de Wiele, T., Vanhaecke, L., Boeckaert, C., Peru, K., Headley, J., Verstraete, W. and  
470 Siciliano, S., 2005. Human colon microbiota transform polycyclic aromatic hydrocarbons  
471 to estrogenic metabolites. *Environmental Health Perspectives* 113, 6-10.

472 Voice, T.C. and Weber, W.J., 1983. Sorption of hydrophobic compounds by sediments, soils  
473 and suspended-solids-1. Theory and background. *Water Res.* 17, 1433-1441.

474 Wang, H.S., Liang, P., Kang, Y., Shao D.D., Zheng, G.J., Wu, S.C., Wong, C.K.C. and Wong,  
475 M.H., 2010. Enrichment of polycyclic aromatic hydrocarbons (PAHs) in mariculture  
476 sediments of Hong Kong. *Environ. Pollut.* 158, 3298-3308.

477 Wang, P. and Keller, A.A., 2009. Partitioning of hydrophobic pesticides within a  
478 soil-water-anionic surfactant system. *Water Res.* 43, 706-714.

479 Wang, X.L., Guo, X.Y., Yang, Y., Tao, S. and Xing, B.S., 2011. Sorption mechanisms of  
480 phenanthrene, lindane, and atrazine with various humic acid fractions from a single soil  
481 sample. *Environ. Sci. Technol.* 45, 2124-2130.

482 Weber, W.J., Huang, W.L. and LeBoeuf, E.J., 1999. Geosorbent organic matter and its  
483 relationship to the binding and sequestration of organic contaminants. *Colloid. Surface. A*  
484 151, 167-179.

485 Wu, W.L. and Sun, H.W., 2010. Sorption-desorption hysteresis of phenanthrene - Effect of  
486 nanopores, solute concentration, and salinity. *Chemosphere* 81, 961-967.

487 Xing, B.S. and Pignatello, J.J., 1997. Dual-mode sorption of low-polarity compounds in  
488 glassy poly(vinyl chloride) and soil organic matter. *Environ. Sci. Technol.* 31, 792-799.

489 Xing, B.S. and Pan, B., 2010. Competitive and complementary adsorption of bisphenol A and  
490 17 alpha-ethinyl estradiol on carbon nanomaterials. *J. Agr. Food Chem.* 58, 8338-8343.

491 Xu, X.R., Wang, Y.X. and Li, X.Y., 2008. Sorption behavior of bisphenol A on marine  
492 sediments. *J. Environ. Sci. Heal. A* 43, 239-246.

493 Xu, J., Yin, K., Lee, J.H.W., Liu, H., Ho, A.Y.T., Yuan, X. and Harrison, P.J., 2010.  
494 Long-term and seasonal changes in nutrients, phytoplankton biomass, and dissolved  
495 oxygen in Deep Bay, Hong Kong. *Estuar. Coast.* 33, 399-416.

496 Yamamoto, H., Liljestrand, H.M., Shimizu, Y. and Morita, M., 2003. Effects of  
497 physical-chemical characteristics on the sorption of selected endocrine disruptors by  
498 dissolved organic matter surrogates. *Environ. Sci. Technol.* 37, 2646-2657.

499 Yang, Y., Zhang, N., Xue, M. and Tao, S., 2010. Impact of soil organic matter on the  
500 distribution of polycyclic aromatic hydrocarbons (PAHs) in soils. *Environ. Pollut.* 158,  
501 2170-2174.

502 Zhao, Q., Weise, L., Li, P.J., Yang, K., Zhang, Y.Q., Dong, D.B., Li, P. and Li, X.J., 2010.  
503 Ageing behavior of phenanthrene and pyrene in soils: A study using sodium  
504 dodecylbenzenesulfonate extraction. *J. Hazard. Mater.* 183, 881-887.

Table 1 - Chemical properties of the selected micropollutants: BPA, EE2, and Phe (Sun et al., 2011).

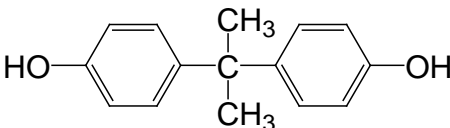
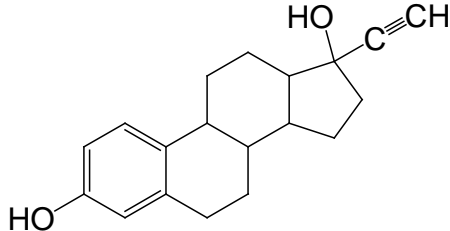
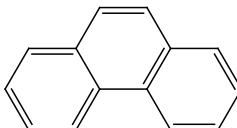
	BPA	EE2	Phe
Molecular structure			
Molecular diameter (Å)	4.3	6.0	5.6
Water solubility, $S_w$ (mg/L)	380	7.6	1.12
Octanol-water distribution coefficient, $\text{Log}K_{ow}$	2.20	4.15	4.57

Table 2 - Summary of the adsorption and desorption isotherms of BPA, EE2, and Phe for the sediment after various periods of incubation.

Chemicals	Incubation time (d)	Adsorption					Desorption		
		Linear model		Freundlich model			Linear model		Hysteresis index (HI, %)
		$K_d$ (L/kg)	$R^2$	Log $K_F$	$1/n$	$R^2$	$K_d$ (L/kg)	$R^2$	
BPA	Raw sediment	4.15±0.15	0.99	1.07±0.022	0.71±0.021	1.00	6.71±0.53	0.97	61.69
	0	34.88±0.76	0.99	1.56±0.021	0.97±0.019	1.00	41.07±0.93	0.99	17.75
	15	26.69±0.86	0.98	1.49±0.043	0.94±0.042	0.99	33.17±1.75	0.97	24.28
	33	16.07±0.29	0.99	1.26±0.029	0.94±0.031	1.00	24.71±1.29	0.97	53.76
	54	12.93±0.34	0.99	1.25±0.024	0.89±0.024	1.00	19.20±0.45	0.99	48.49
	75	12.31±0.21	1.00	1.18±0.022	0.92±0.017	1.00	19.67±1.38	0.95	59.79
	96	13.54±0.31	0.99	1.22±0.031	0.92±0.032	1.00	22.41±1.47	0.96	65.51
	125	10.60±0.17	0.99	1.16±0.018	0.89±0.02	1.00	18.08±1.70	0.92	70.57
EE2	Raw sediment	25.27±0.98	0.97	1.48±0.009	0.77±0.022	0.99	9.83±0.95	0.89	-
	0	100.08±3.74	0.95	2.02±0.018	1.02±0.079	0.97	45.18±3.12	0.85	-
	15	89.94±2.67	0.97	1.95±0.020	1.12±0.072	0.98	45.49±1.69	0.96	-
	33	61.40±1.94	0.96	1.81±0.019	0.99±0.074	0.97	25.53±1.21	0.93	-
	54	57.49±1.39	0.98	1.75±0.012	1.07±0.049	0.99	22.28±1.99	0.76	-
	75	59.82±1.81	0.97	1.82±0.022	0.91±0.063	0.97	23.77±2.09	0.76	-
	96	63.02±1.53	0.98	1.82±0.019	1.00±0.055	0.98	27.30±1.73	0.87	-
	125	73.05±2.63	0.98	1.80±0.027	1.33±0.11	0.96	26.95±1.98	0.84	-
Phe	Raw sediment	132.5±3.3	0.98	1.98±0.038	1.13±0.049	0.99	6.47±0.74	0.92	-



0	4430±168	0.95	3.66±0.19	1.02±0.18	0.93	36.00±1.49	0.98	-
15	5612±66	1.00	3.84±0.039	1.08±0.029	1.00	-	-	-
33	4962±158	0.98	3.95±0.12	1.24±0.10	0.98	36.49±2.28	0.97	-
54	4686±178	0.99	4.17±0.056	1.47±0.057	1.00	-	-	-
75	4731±182	0.99	4.20±0.068	1.49±0.057	1.00	47.58±1.83	0.96	-
96	4988±312	0.98	4.95±0.27	2.16±0.25	0.97	-	-	-
125	4916±264	0.95	4.27±0.24	1.54±0.22	0.95	51.59±4.47	0.95	-

---

“-”: invalid or not determined.

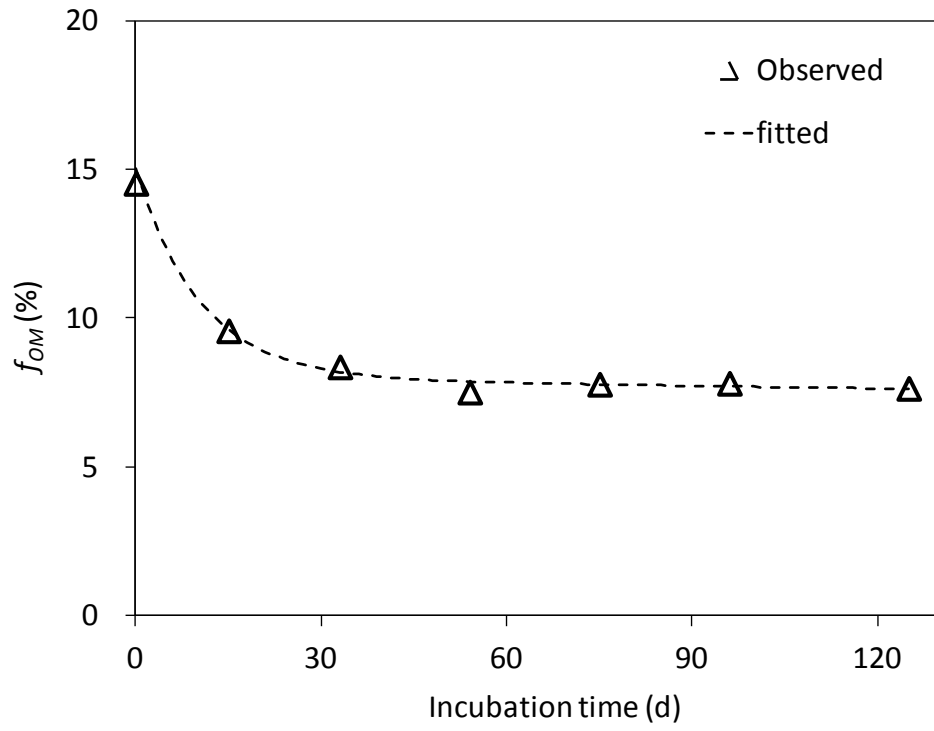


Fig. 1 - SOM reduction during the sediment incubation.

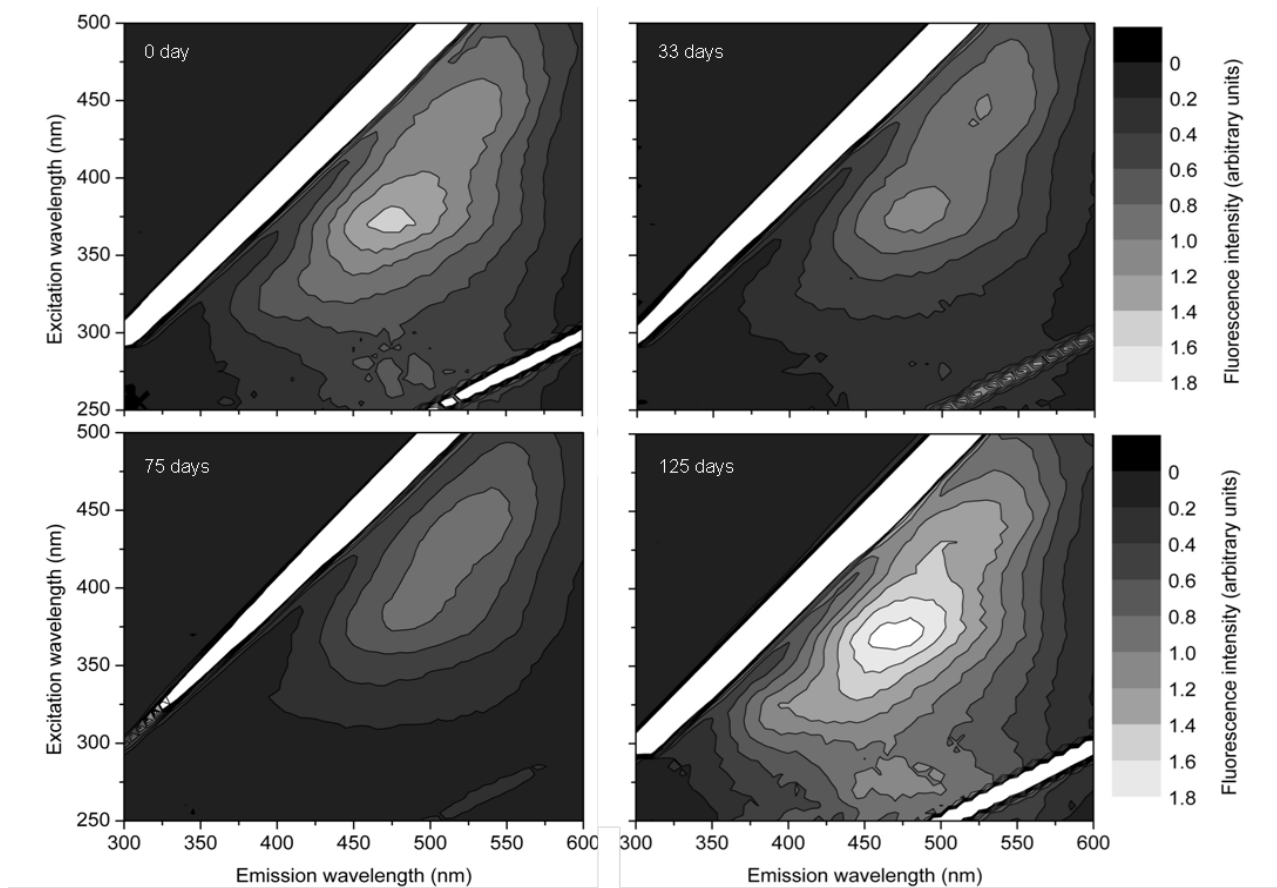


Fig. 2- FEEM of the humic substances extracted from the sediment samples after different incubation periods.

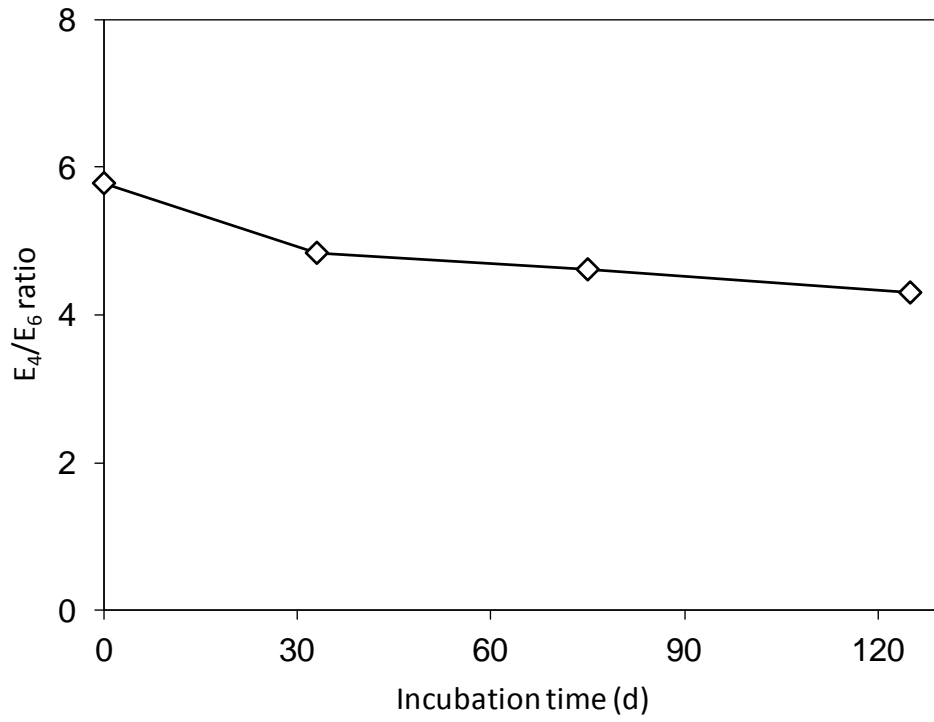


Fig. 3- E<sub>4</sub>/E<sub>6</sub> ratio of the humic substances extracted from the sediment samples after different periods of sediment incubation.

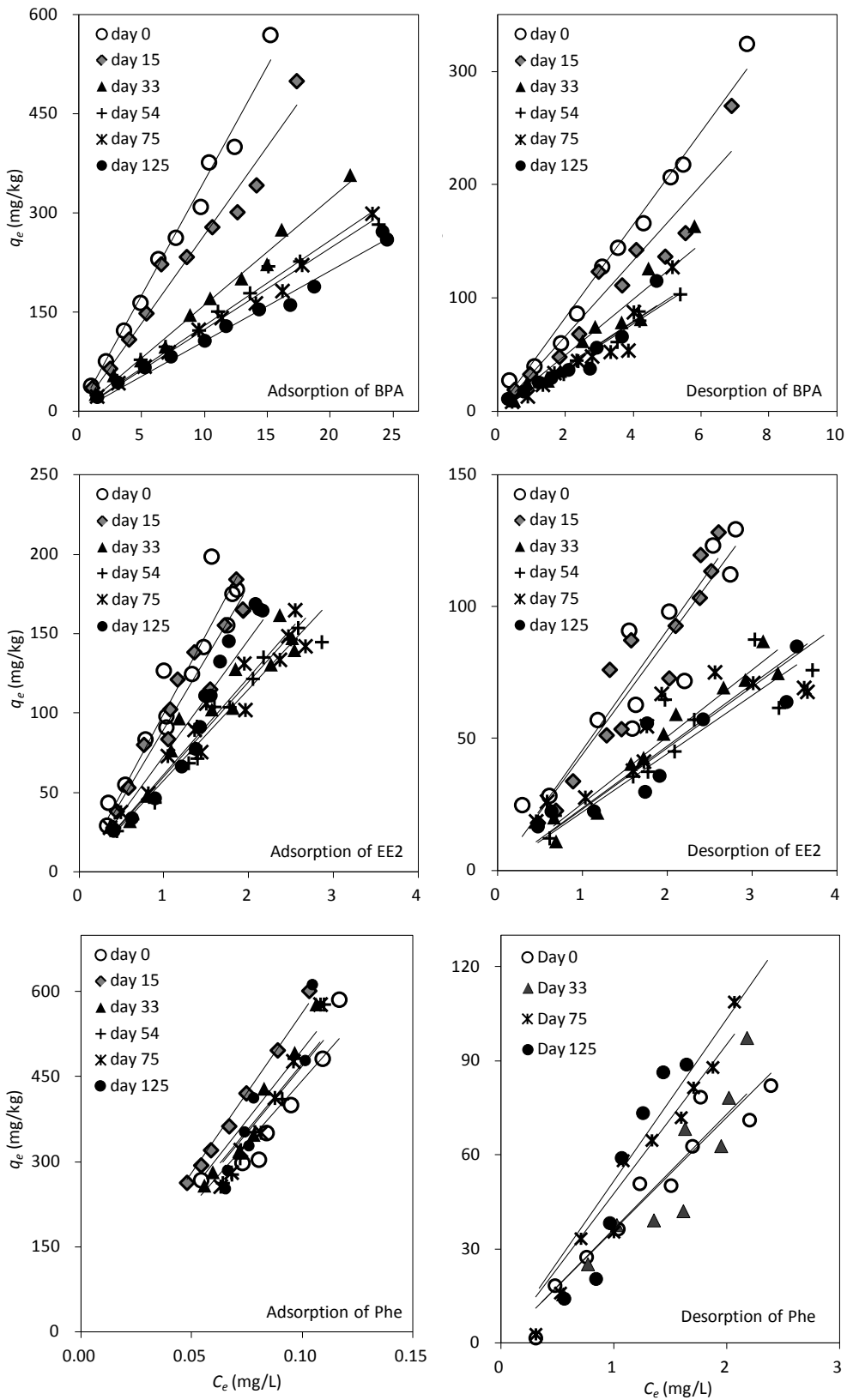


Fig. 4 - Isotherms of the adsorption and desorption of BPA, EE2, and Phe for the sediment samples after different periods of incubation.

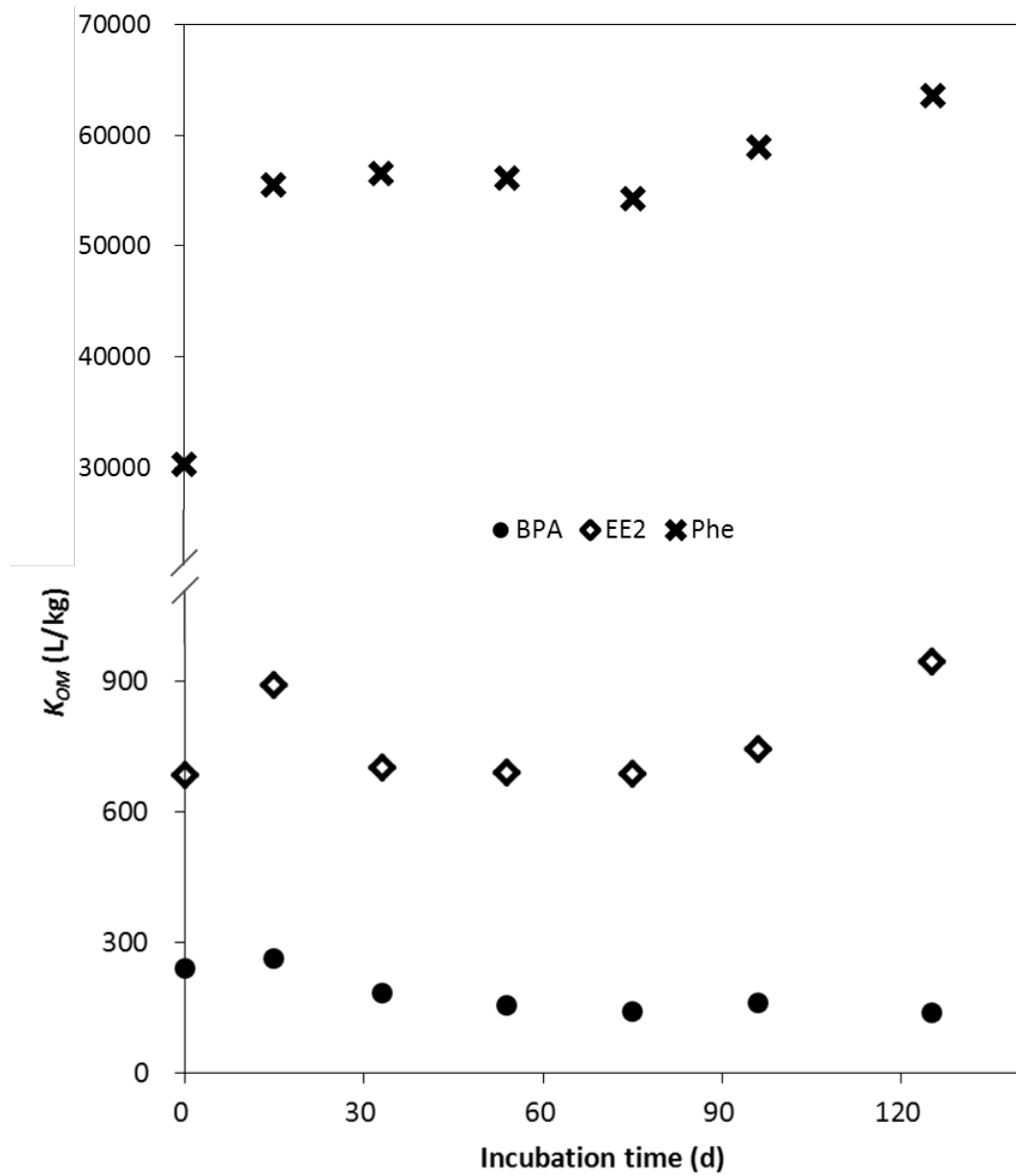


Fig. 5 - Changes in the  $K_{OM}$  values of BPA, EE2, and Phe with the sediment incubation time.

1 **Supplementary Material**

2

3 **Changes in the adsorption of bisphenol A, 17  $\alpha$ -ethinyl estradiol,**  
4 **and phenanthrene on marine sediment in Hong Kong in relation**  
5 **to the simulated sediment organic matter decomposition**

6

7 **Ying-heng Fei<sup>1, 2</sup>, Baoshan Xing<sup>3</sup>, Xiao-yan Li<sup>1\*</sup>**

8 <sup>1</sup> Department of Civil Engineering, The University of Hong Kong, Hong Kong, China

9 <sup>2</sup> Water Science Research Center, Guangzhou Institute of Advanced Technology, Chinese  
10 Academy of Sciences, Guangzhou, China

11 <sup>3</sup> Department of Plant, Soil and Insect Sciences, University of Massachusetts, Amherst,  
12 MA, USA

13 (\*Corresponding author: phone: 852-28592659; fax: 852-28595337; e-mail: xlia@hkucc.hku.hk)

14  
15 The following supplementary materials are included:

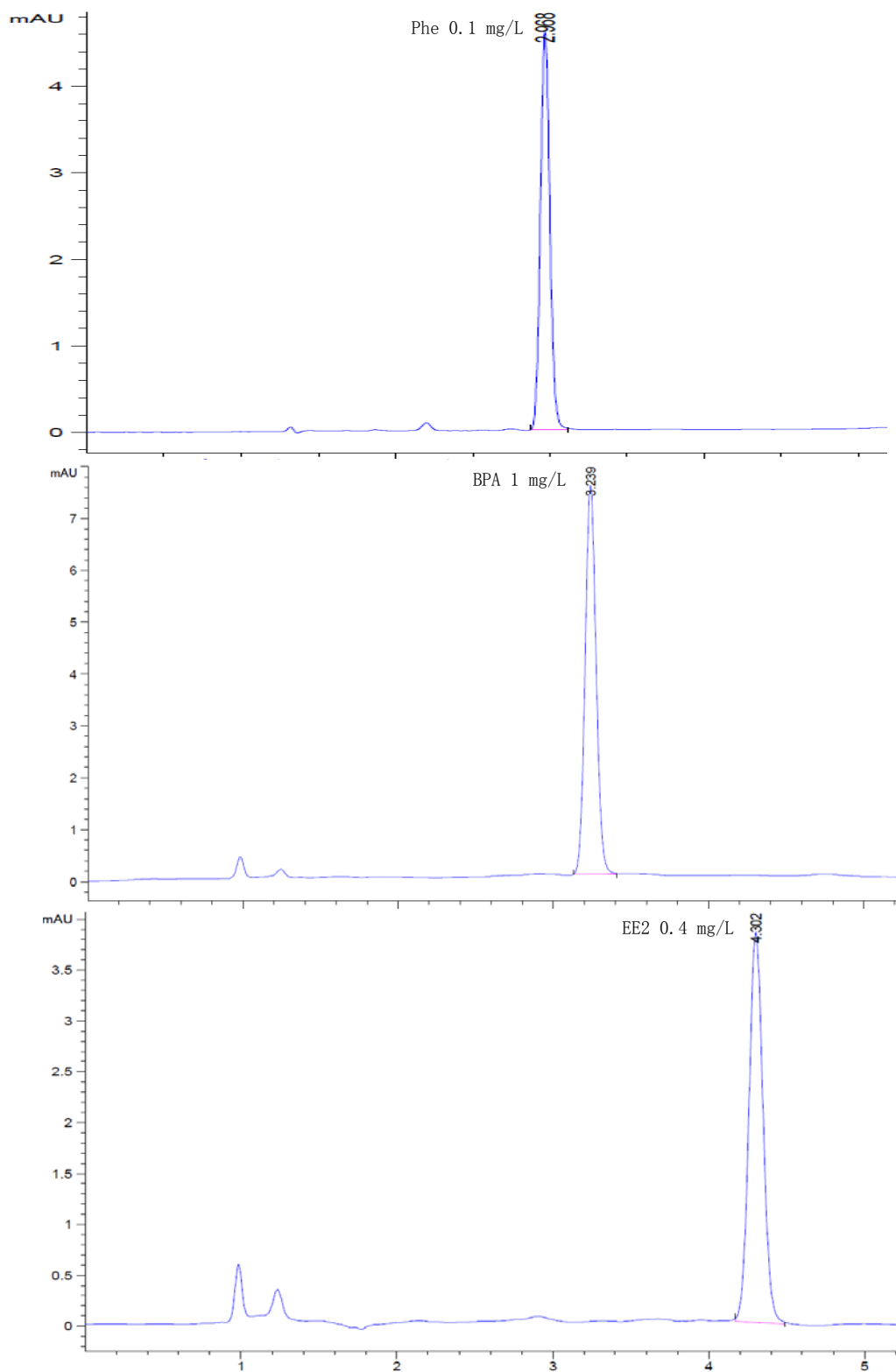
16 (1) HPLC chromatograph for BPA, EE2 and Phe detection.

17 (2) A conceptual model for SOM decay in sediment and its effect on adsorption capacity.

18

19 (1) HPLC chromatograph for BPA, EE2 and Phe detection

20



21

22

Fig. S1 - HPLC chromatograph for BPA, EE2 and Phe detection.

23



24 **(2) A conceptual model for SOM decay in sediment and its effect on adsorption**  
25 **capacity**

26

27 The lab results reveal that fresh particulate matter deposited into sediment may not  
28 behave as a stable entity for the transport of pollutants in the environment. SOM will undergo  
29 various forms of degradation and diagenesis, and the aging process will alter the chemical  
30 adsorption capacity of the sediment. However, in conventional chemical partition modeling  
31 concerning SOM, a simple model of  $K_d = f_{OM} K_{OM}$  is often used, in which all SOM  
32 contents are grouped into the  $f_{OM}$  fraction with a single  $K_{OM}$  value. This study shows that such  
33 a simplified approach cannot be employed to describe the dynamics of SOM degradation and  
34 the resulting changes in adsorption capacity. It may be necessary to adopt a multi-fractional  
35 approach to describe SOM transformation and its effect on sediment adsorption.

36 SOM input into sediment consists of multiple components in terms of biodegradability,  
37 ranging from readily biodegradable organic matter to less degradable, refractory and  
38 non-degradable organics (deBruyn and Gobas, 2004). Hence, the  $f_{OM}$  fraction can be written  
39 as the sum of the finer individual SOM fractions, i.e.

40 
$$f_{OM} = \sum_{i=1}^n f_{OM_i} \quad (S1)$$

41 where  $i$  signifies the  $i^{\text{th}}$  SOM fraction. The fraction  $f_{OM1}$  represents the most readily  
42 biodegradable organic fraction, and as the  $i$  value increases, the SOM fraction becomes less  
43 degradable.

44 In this experimental study, initial  $f_{OM}$  in the sediment was around 15%, including 5% of  
45 raw organic in the Harbour sediment and 10% of fish food (SOM) added into the sediment.  
46 Most of the raw SOM in the natural sediment could be considered refractory, while feeds in  
47 the fish farms are usually believed to be predominated by labile organic matters (deBruyn and

48 Gobas, 2004). For the loaded fish food pellets that contains about 70% of proteins and lipids,  
 49 and 30% of fibers and other carbohydrates, based on the product information, the fast- and  
 50 slow-decomposing fractions with a ratio of 7:3 might be assumed (Jamu and Piedrahita, 2002;  
 51 Arndt et al., 2013). Hence, the initial  $f_{OM}$  could be approximated into 3 components with a  
 52 ratio of 7:3:5.

53 Assuming first-order kinetics for the degradation of different organic components in  
 54 sediment, the fraction-based SOM reduction dynamics may be described by the following  
 55 simplified form:

$$56 \quad f_{OM}^t = \sum_{i=1}^n f_{OM_i}^0 e^{-k_i t} \quad (S2)$$

57 where  $f_{OM}^t$  is the overall SOM content after period  $t$ ,  $f_{OM_i}^0$  stands for the  $i^{\text{th}}$  fraction of fresh  
 58 SOM on day 0, and  $k_i$  is the rate constant of organic degradation for the  $i^{\text{th}}$  SOM fraction.  
 59 Using the best fit for the SOM reduction results reported in Fig. S1 as an example, the  
 60 following expression can be obtained for SOM degradation during sediment incubation:

$$61 \quad f_{OM}^t = 0.07e^{-0.096t} + 0.03e^{-0.0011t} + 0.05e^{-0t} \quad (S3)$$

62 This fitting result is comparable to organic decomposition rates observed by others. For  
 63 instance, it has been reported that rapid and slow organic decay occur in the order of several  
 64 per cents and tenths of a per cent per day in marine sediment, respectively, while recalcitrant  
 65 organic substances in sediment can decay at the rate of 0.1% per year or lower (deBruyn and  
 66 Gobas, 2004).

67 In relation to the SOM fractions, there should be a  $K_{OM}$  value for the adsorption of a  
 68 given chemical pollutant by a particular  $f_{OM}$  fraction. Thus, the SOM-based partition  
 69 coefficient may be written as

$$70 \quad K_d = \sum_{i=1}^n f_{OM_i} K_{OM_i} \quad (S4)$$

71 Furthermore, the overall  $K_{OM}$  value, or  $K_d/f_{OM}$ , can be calculated by

$$72 \quad K_{OM} = \sum_{i=1}^n \frac{f_{OM_i}}{f_{OM}} K_{OM_i} \quad (S5)$$

73 For each fraction, the fractional coefficient,  $K_{OM_i}$ , is a constant, as for that unchanged  
74 chemical composition and structure is assumed for each subdivided fraction. Hence, the  
75 change of SOM during organic composition was achieved by the alteration among different  
76 fractions, instead of the chemical transformation inside each fraction. When SOM undergoes  
77 humification, many SOM fractions, particularly the readily biodegradable fractions, i.e.  $f_{OM1}$ ,  
78  $f_{OM2}$  or  $f_{OM3}$ ..., will reduce over time. Thus, there could be a shift in the  $f_{OM_i}$  profile during the  
79 sediment aging process. The  $f_{OM_i}$  for lower  $i$  SOM fractions will decrease significantly, and  
80 the  $f_{OM_i}$  for the higher  $i$  fractions will hardly decrease and may even increase. As a result, the  
81  $f_{OM_i}/f_{OM}$  ratio will decrease greatly for lower  $i$  fractions and will increase considerably for  
82 higher  $i$  fractions. In the present study, after 120 d of incubation the fractional ratio of  $f_{OM}$   
83 shifted to 0:2.5:5. As we can find out that, not only the SOM content decreased from 15% to  
84 7.6%, and also the SOM fraction distribution was altered from  $f_{OM1}$  dominated to  $f_{OM3}$   
85 dominated.

86 The change in the  $f_{OM_i}$  profile during sediment aging will affect the chemical adsorption  
87 capacity of the sediment. In comparison to more hydrophilic and biodegradable SOM, more  
88 condensed humic-like SOM bring about more and stronger adsorption (Sun et al., 2010;  
89 Weber et al., 1999). Thus, for hydrophobic micropollutants typically found in sediment,  $K_{OM_i}$   
90 values for lower  $i$  SOM fractions are generally lower than those for higher  $i$  fractions. If the  
91 difference is only marginal for a particular chemical, i.e.  $K_{OM_i} \approx K_{OM_j}$  ( $i < j$ ), Eq. S5 suggests  
92 that the change in the  $f_{OM_i}$  profile resulted from the SOM degradation will cause little change  
93 in the overall  $K_{OM}$  value of the sediment. This is likely to have been the case for hydrophilic  
94 chemicals, i.e. BPA observed in this study. However, SOM decay and reduction would still

95 lead to a continuous decrease in the  $K_d$  value of BPA in the sediment. If the difference is  
96 significant, i.e.  $K_{OMi} < K_{OMj}$  ( $i < j$ ), the change in the  $f_{OMi}$  profile will result in a general  
97 increase in the overall  $K_{OM}$  value, which is likely to have been the case for EE2 and Phe  
98 observed here. If the difference is rather great, i.e.  $K_{OMi} \ll K_{OMj}$  ( $i < j$ ), the change in the  $f_{OMi}$   
99 profile would lead to a greater increase in  $K_{OM}$ . Moreover, the overall  $K_d$  value may not  
100 decrease but increase with the SOM decay and  $f_{OM}$  reduction, as displayed by both Phe and  
101 EE2 in the later phase of sediment incubation.

102 The model proposed here is basically a conceptual description for the analysis of  
103 experimental observations on the change in chemical adsorption by sediment in relation to  
104 SOM degradation. The great complexity of sediment and the dynamic changes in SOM  
105 components mean determining  $f_{OMi}$  fractions and corresponding  $K_{OMi}$  values is extremely  
106 difficult, if not impossible. To quantitatively validate it to a mathematical model, the SOM  
107 fractionation as well as the determination of the assigned fractional  $K_{OM}$  need to be further  
108 discussed, and the dynamic change of each fraction need to be carefully monitored. This  
109 would be a follow-up study in the future. Nonetheless, the model and its underlying  
110 mechanism provide a sound basis for predicting the impact of organic deposition and SOM  
111 decomposition on the adsorption of environmental pollutants in marine sediment.

112

### 113 **References:**

- 114 Arndt, S., Jorgensen, B.B., LaRowa, D.E., Middelburg, J.J., Pancost, R.D. and Regnier, P.,  
115 2013. Quantifying the degradation of organic matter in marine sediments: A review and  
116 synthesis. *Earth-Sci. Rev.* 123, 53-86.
- 117 deBruyn, A.M.H. and Gobas, F.A.P.C., 2004. Modelling the diagenetic fate of persistent  
118 organic pollutants in organically enriched sediments. *Ecol. Model.* 179, 405-416.

119 Jamu, D.M. and Piedrahita, R.H., 2002. An organic matter and nitrogen dynamics model for  
120 the ecological analysis of integrated aquaculture/agriculture system: I. model  
121 development and calibration. *Environ. Modell. Softw.* 17, 571-582.

122 Sun, K., Gao, B., Zhang, Z.Y., Zhang, G.X., Liu, X.T. Zhao, Y. and Xing, B.S., 2010.  
123 Sorption of endocrine disrupting chemicals by condensed organic matter in soils and  
124 sediments. *Chemosphere* 80, 709-715.

125 Weber, W.J., Huang, W.L. and LeBoeuf, E.J., 1999. Geosorbent organic matter and its  
126 relationship to the binding and sequestration of organic contaminants. *Colloid Surface A*  
127 151, 167-179.

128